Analytica Chimica Acta 1128 (2020) 231–237

Contents lists available at ScienceDirect

Analytica Chimica Acta

journal homepage: www.elsevier.com/locate/aca

Organic electrochemical transistor for sensing of sialic acid in serum samples

Lizhen Chen [a], Naixiang Wang [b], Jie Wu [a], Feng Yan [b], Huangxian Ju [a, *]

[a] State Key Laboratory of Analytical Chemistry for Life Science, School of Chemistry and Chemical Engineering, Nanjing University, Nanjing, 210023, China
[b] Department of Physics, The Hong Kong Polytechnic University, Hong Kong

HIGHLIGHTS

- The biosensor based on organic electrochemical transistor is designed for detection of sialic acid in serum samples.
- The recognition of sialic acid to aminophenylboronic acid on gate electrode leads to the change of channel current.
- The designed biosensor shows excellent selectivity toward sialic acid.
- The biosensor realizes the evaluation of sialic acid levels in practical sample analysis.

GRAPHICAL ABSTRACT

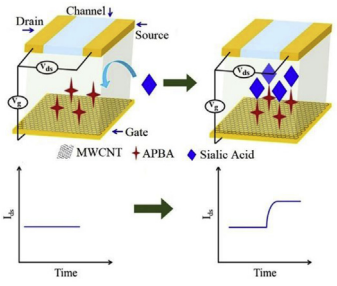

ARTICLE INFO

Article history:
Received 9 June 2020
Received in revised form
30 June 2020
Accepted 2 July 2020
Available online 13 July 2020

Keywords:
Organic electrochemical transistor
Sialic acid
Biosensor
Boronic acid

ABSTRACT

Sialic acid usually locates at the terminal of glycoproteins and glycolipids on cell surface. Compared to normal cells, cancer cells generally express much more sialic acid residues, and the sialylation of cell surface proteins or lipids is related to the progression of tumors, which leads to high expression of serum sialic acid in cancer patients. This work used an organic electrochemical transistor as the sensing platform to design a simple and suitable device for sensitive and convenient detection of sialic acid level in serum samples. The transistor-based biosensor consisted of three typical drain/source/gate Au electrodes on a glass substrate and a polymer membrane to serve as conducting channel between source electrode and drain electrode. The gate electrode was modified with carboxylated multi-wall carbon nanotubes to covalently bind 3-aminobenzeneboronic acid, which specifically recognized sialic acid to change the effect gate voltage of the transistor, and thus produced the signal of drain-source channel current for sensitive detection of sialic acid ranging from 0.1 to 7 mM. The novel biosensor possessed excellent specificity for distinguishing normal and cancer people. The detection results of serum samples from lung cancer patients demonstrated the excellent performance of the transistor-based biosensor, showing the potential application in clinical diagnose.

1. Introduction

Glycans and glycoproteins are involved in many physiological processes such as proliferation, differentiation, growth and apoptosis [1–5]. Sialic acid (SA) usually locates at the nonreducing terminal of the glycoproteins and glycolipids on cell surface [6,7].

* Corresponding author.
E-mail address: hxju@nju.edu.cn (H. Ju).

https://doi.org/10.1016/j.aca.2020.07.006
0003-2670/

When normal cells pathologically change, the glycolipids and glycoproteins on cell membrane are vast synthesized and abnormally transformed, which leads to the overexpression of SA residues on cell surface and high SA level in serum samples of tumor patients. Many reports have indicated that the SA level in blood serum is closely related to the occurrence, development and transfer of tumors [8–11]. Therefore, SA has been adapted as a kind of biomarker for clinical tumor diagnosis [12–15], and many methods have been established for the detection of serum sialic acid level by using surface-enhanced Raman scattering [16,17], colorimetric [18], quartz crystal microbalance [19], localized surface plasmon resonance [20], liquid chromatography-tandem mass spectrometric [21] and electrochemical [22–25] techniques. The enzyme linked immunosorbent assay (ELISA) kit has also been commercialized for this purpose. Although some methods are highly sensitive, they have still some disadvantages such as complex pretreatment of blood samples or multiple dilution. Thus sensitive and convenient biosensing methods for detection of sialic acid level in serum samples are still in urgent demand.

Organic electrochemical transistors (OECTs), as a new generation of sensing platforms, have shown great potential in biodetection applications [26,27]. The OECT is typically consisted of three electrodes named drain, source, gate electrodes respectively, and a conducting channel, which connects the drain and source electrodes and can be prepared with conductive polymers. The poly(3,4-ethylenedioxythiophene) doped with poly(styrene sulfonate) (PEDOT:PSS) has been widely used as the channel polymer owing to its stability, biocompatibility and high conductivity. Usually, the OECTs show high sensitivity under relatively low working voltage (less than 1 V) [28,29]. Moreover, the OECT devices are low-cost, easy to fabricate, biocompatible and flexible. Thus it is promising to develop the portable OECT based biosensors for sensitive and convenient detection of biomolecules. Some researchers have used OECTs as sensing platform to propose several devices for monitoring of human biological signals [30–33]. The OECT-based biosensors have also been reported for the detections of electrochemically active molecules such as hydrion [34], dopamine [35], uric acid [36], glucose [37,38], epinephrine [39], gallic acid [40], amino acid [41] and acetylcholine [42], due to the change of the effect gate voltage of the transistor upon the occurrence of electron transfer between the target molecules and gate electrode, which sensitively changes the drain-source channel current. Interestingly, the interaction between gate electrode and some inactive molecules, macromolecules or small particles, such as cortisol [43], DNA [44], proteins [45], bacteria [46], cell [47], antibody [48] and glycans [49], can also change the effect gate voltage of the transistor through different mechanisms to produce the drain-source channel current signal. Thus the corresponding OECT-based biosensors have been widely reported.

In this paper, we proposed a simple strategy for the preparation of specific OECT-based biosensor. The basic constitution of the OECTs was drain/source/gate electrodes made with chromium/gold thin layer and the PEDOT:PSS membrane that covered on drain/source area to serve as conducting channel. To achieve the specific detection of sialic acid level in clinical serum samples, 3-aminophenylboronic acid (APBA) that can quickly link 1,2- or 1,3-diols of monosaccharides by boronic acid-based ligation [50,51] was bounded on gate electrode surface with carboxylated multi-wall carbon nanotubes (MWCNT-COOH). Upon the specific binding of SA to APBA covalently immobilized on the gate electrode, the electron transfer impedance increased greatly, which changed the voltage between the electrolyte/channel and gate/electrolyte interfaces, thus caused the change of drain-source channel current. The advantages of OECTs and the excellent performance of the designed OECT-based biosensor for the detection of SA level in practical serum samples demonstrated its great potential in clinical application.

2. Experimental

2.1. Materials and reagents

Multi-wall carbon nanotubes (MWCNTs) were supplied by XFNANO Materials Tech Co., Ltd (Nanjing, China). APBA, SA, 1-(3-dimethylaminopropyl)-3-ethylcarbodiimide hydrochloride (EDC) and N-hydroxysuccinimide (NHS) were purchased from Sigma-Aldrich (USA). PEDOT:PSS (Clevios™, PH 1000) was provided by Heraeus (Germany). Acetone, isopropanol, dimethylsulfoxide (DMSO), glycerin, Tween 20, nitric acid and sulfuric acid with analytical grade were produced by Sinopharm Chemical Reagent Co., Ltd (Shanghai, China). The photoresist with its developer (AZ514) and the metal etchant were purchased from Suzhou Cchip Scientific Instrument Co., Ltd (China). The commercial ELISA kit for SA detection was purchased from Jin Yibai Biological Technology Co., Ltd (Nanjing, China).

2.2. Apparatus

The drain-source channel currents were measured by connecting the three electrodes to Keysight B1500A semiconductor analyzer (USA). The Zeta potentials were measured using a 90 Plus DynaPro NanoStar (Brookhaven Instrument Corporation, USA). The electrochemical impedance spectra (EIS) were obtained from the Princeton Parstat MC 1000 (USA). Kurt J. Lesker PVD75 E-beam evaporation system (USA) was used to deposit the Cr/Au layer on glass substrate. The lithography process was accomplished on SUSS MA6-SCILL mask aligner along with a nanoimprinting system (Germany). The Harrick plasma cleaner PDC-002 was used for oxygen plasma treatment (USA). The KW-4A spin-coater was provided by Beijing SETCAS Electronics Co., Ltd (China). Scanning electron microscope (SEM) (JEOL Model JSM-6490, Japan) was used to characterize the nanomaterials and the biological modification on the gate electrode.

2.3. Fabrication of OECT

The OECT was prepared with a typical pattern method, as shown in Fig. 1A. In brief, the Cr adhesion layer and the Au layer were successively deposited on a glass substrate by E-beam evaporation. The total size of the device was 1.1 cm × 1.2 cm, and the thickness of Cr and Au layers were 10 and 100 nm, respectively. The three electrodes were patterned through a lithography way using positive photoresist (AZ514) and the designed photomask. The Au gate electrode was set as 1 × 1 mm^2, 2 × 2 mm^2 and 3 × 3 mm^2, respectively. After the patterned device was washed with acetone and treated with oxygen plasma, PEDOT:PSS solution containing 5% glycerin and 5% DMSO (V/V) was spin-coated on the device at 3600 rpm for 35 s to form a thin film, following an annealing process in vacuum drying oven at 120 °C for 1 h. The conducting channel covered on drain/source area was formed by dissolving the PEDOT:PSS film coated on other area with isopropanol in the help of protection tape. The width and length of the OECT channel were 0.2 and 6 mm, respectively.

2.4. Modification of gate electrode

MWCNTs were firstly pretreated with the mixture of HNO_3/H_2SO_4 (1:3 V/V) by refluxing overnight at 140 °C. The mixture was centrifuged at 13,000 rpm for 15 min and washed with 0.01% V/V Tween 20 till the pH of final washing solution was neutral. The

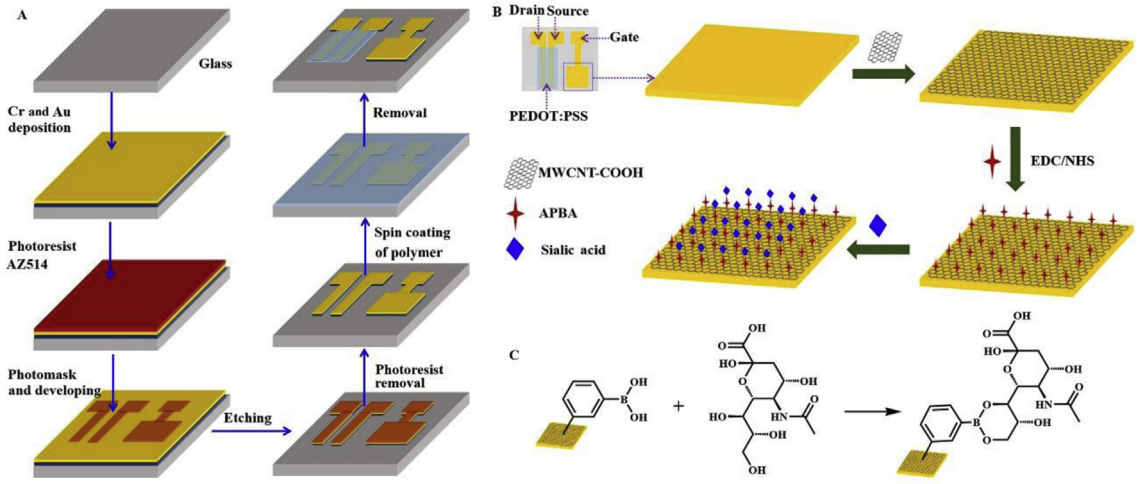

Fig. 1. Schematic illustration of (A) OECT fabrication, (B) OECT-based biosensor preparation and sialic acid sensing. (C) Recognition reaction between APBA and SA on biosensor surface.

expected carboxylated MWCNTs (MWCNT-COOH, named CNT) was re-dispersed as 1 mg/mL dispersion for future use.

9 μL of CNT dispersion was dropped on gate electrode (3×3 mm^2) surface to form a firm thin film at room temperature (Fig. 1B). Then 9 μL of the mixture of 5 mM EDC and 5 mM NHS was dropped on the CNT modified gate electrode and incubated at 4 °C for 4 h to activate the carboxyl groups. Finally, 9 μL of 50 mM APBA solution was dropped on the gate electrode for another 2 h at 37 °C to covalently immobilize APBA on the gate electrode. After rinsing the modified gate electrode with pH 7.4 phosphate buffered solution (PBS), the specific OECT-based biosensor for SA was obtained. To keep the same loading capacity on unit area, 4 and 1 μL of above dispersion or solution were dropped on the gate electrodes with area of 4 and 1 mm^2 for biosensor preparation, respectively. The biosensor was examined with the transfer curve at a drain voltage of 50 mV as the gate voltage varied from 0 V to 1.2 V and the source electrode was connected to ground, representing the source voltage was zero.

2.5. Sialic acid detection

10 mM pH 7.4 PBS containing sialic acid was used for measurements of drain-source channel current. After 10-min incubation, the drain-source channel current was recorded as a time function at a gate voltage of 0.9 V, while the drain voltage was fixed at 50 mV, and the source electrode was connected to ground. The steady response at 300 s was used for SA detection.

3. Results and discussion

3.1. Design of OECT-based SA biosensor

To achieve the specific detection of sialic acid, this work firstly immobilized APBA on gate electrode surface for the preparation of OECT-based biosensor. Upon the addition of sialic acid sample, the immobilized APBA could quickly recognize the target molecule by boronic acid-based ligation to 1,3-diols of SA (Fig. 1C). The immobilization of APBA was performed by covalently linking the $-NH_2$ group to activated carboxyl group of carboxylated MWCNTs film in the presence of EDC and NHS (Fig. 1B). The large specific surface area and excellent electrical property of MWCNTs provided the advantages for loading of APBA and highly sensitive detection of electronic signal for SA. Upon the specific binding of SA to APBA on gate electrode, the electron transfer impedance increased greatly, which caused the voltage change between the electrolyte/channel and gate/electrolyte interfaces, and thus the variation of drain-source channel current. Here the recognition process influenced the electron transfer impedance of the gate electrode, which indicated that the proposed OECT-based biosensor worked in the non-Faradaic regime [25,52].

3.2. Characterization of modified gate electrode

The Zeta potentials were firstly detected to examine the charge change during the continuous treatments of carbon nanotubes for carboxylation, APBA binding and recognition to sialic acid (Fig. 2A). The pretreatment of MWCNTs with HNO_3/H_2SO_4 could generated carboxyl groups on the surface of carbon nanotubes, thus the Zeta potential became more negative. After the linkage of APBA to MWCNT-COOH (CNT), the presence of negatively charged boronic group led to more negative Zeta potential, which became less

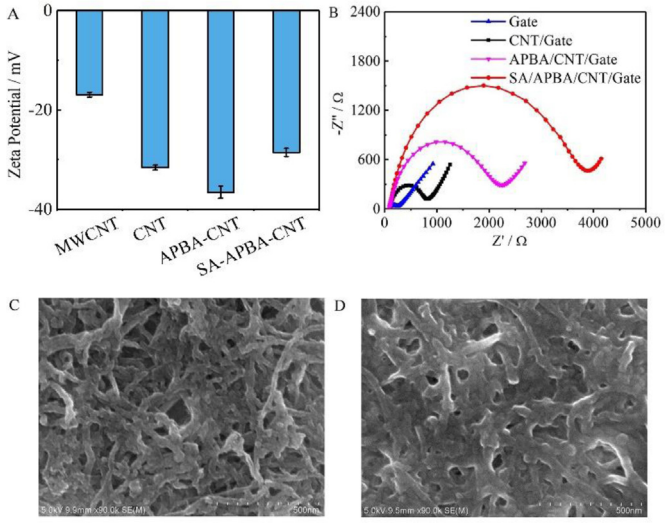

Fig. 2. (A) Zeta potential of MWCNT, CNT, APBA-CNT and SA-APBA-CNT. (B) EIS of bare and different modified gate electrodes in 10 mM pH 7.4 PBS containing 0.1 M KCl and 5 mM $K_4[Fe(CN)_6]/K_3[Fe(CN)_6]$ (1:1). Frequency range: 100 kHz to 0.01 Hz; amplitude: 10 mV. SEM images of (C) CNT and (D) SA/APBA/CNT modified gate electrodes.

negative after the recognition of SA to immobilized APBA owing to the boronic acid-based ligation of SA.

The EIS was also used to confirm the modification process of gate electrode (Fig. 2B). After carboxylated MWCNTs were coated on the gate electrode, the electron-transfer resistance increased due to the repulsion between $K_4[Fe(CN)_6]/K_3[Fe(CN)_6]$ probe and negatively charged electrode surface. After APBA was linked to CNT modified gate surface, the electron-transfer resistance became larger owing to the presence of hydrophobic phenyl group and negatively charged boronic acid at pH 7.4, which blocked the electron transfer and further increased the repulsion between $K_4[Fe(CN)_6]/K_3[Fe(CN)_6]$ and electrode surface, respectively. After the recognition of SA to immobilized APBA, the electron-transfer resistance obviously increased due to the formation of relatively more hydrophobic boric ester and the steric hindrance.

The morphology of the modified gate electrodes were illustrated with the SEM images. When the CNT was dropped on the gate electrode, the surface structure of CNT film was well-dispersed in the form of small bundles or single tubes (Fig. 2C). After the binding of APBA and SA onto CNT modified gate electrode, the surface morphology became slightly rough (Fig. 2D). Since APBA and SA were relatively small molecules, the effective immobilization of APBA and SA on the gate electrode could not cause the obvious change of surface morphology of carbon nanotubes except that the tube structure became plumper.

3.3. Sialic acid detection with OECT-based biosensor

The OECT-based sensor with the gate area of 9 mm^2 showed the typical transfer curve in PBS electrolyte with the channel current change of 1 order of magnitude when the gate voltage varied from 0 to 1.2 V (Fig. 3A). The transconductance, which could be extracted from the differentiation of channel current to gate voltage, reached the maximum value of 0.9 mS at 0.9 V, indicating that the designed transistor-based sensor could show the best performance with the gate voltage of 0.9 V (Fig. 3A).

To further verify above result, the biosensor was tested at the gate voltage of 0.3 V, 0.6 V and 0.9 V in PBS containing different concentrations of SA. Upon the addition of 2.5, 5 and 8 mM SA in PBS, the channel current continuously increased (Fig. 3B), and all the maximum relative channel current changes ($\Delta I/I_0$, here I_0 is the steady channel current measured before the addition of SA in PBS) occurred at 0.9 V (Fig. 3C), which could be used for more sensitive quantitation of SA. Considering the fact that the gate voltages higher than 1 V might influence the service life of the device, and the OECT-based biosensors are generally operated at low voltage (<1 V), it was reasonable to set the working gate voltage of the designed biosensor at 0.9 V.

Under the optimized gate voltage, the drain-source currents were recorded to examine the SA response at different gate electrodes. The device with the APBA/CNT modified gate electrode did not show obvious response toward the PBS, while the addition of 3.0 mM SA in PBS led to great response, which was much greater than that at CNT modified gate electrode to the addition of even 6.0 mM SA (Fig. 3D), indicating the specific recognition of APBA to SA. To obtain the best performance of the designed biosensor, the loading amounts of CNT and APBA on the gate electrode were also optimized to be 1.0 mg/mL and 50 mM, respectively (Fig. 3E and F).

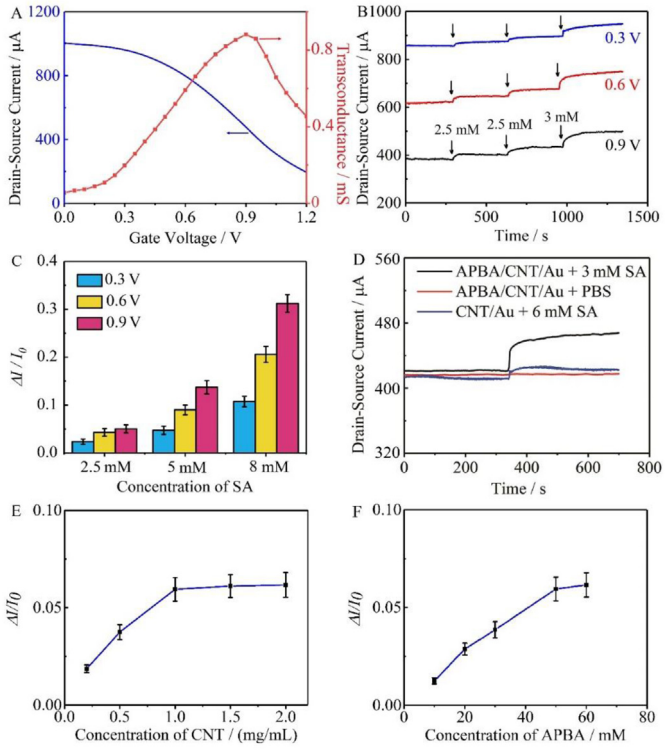

Fig. 3. (A) Transfer and transconductance curves of the OECT-based sensor with PBS as electrolyte. (B) Drain-source channel current responses to SA addition in PBS at different gate voltages. (C) Relative channel current change ($\Delta I/I_0$) toward SA addition at different gate voltages. (D) Response of CNT or APBA/CNT modified gate electrodes to PBS and addition of SA in PBS. (E, F) Current response ($\Delta I/I_0$) at different concentrations of CNT (E) and APBA (F) modified on the gate electrode.

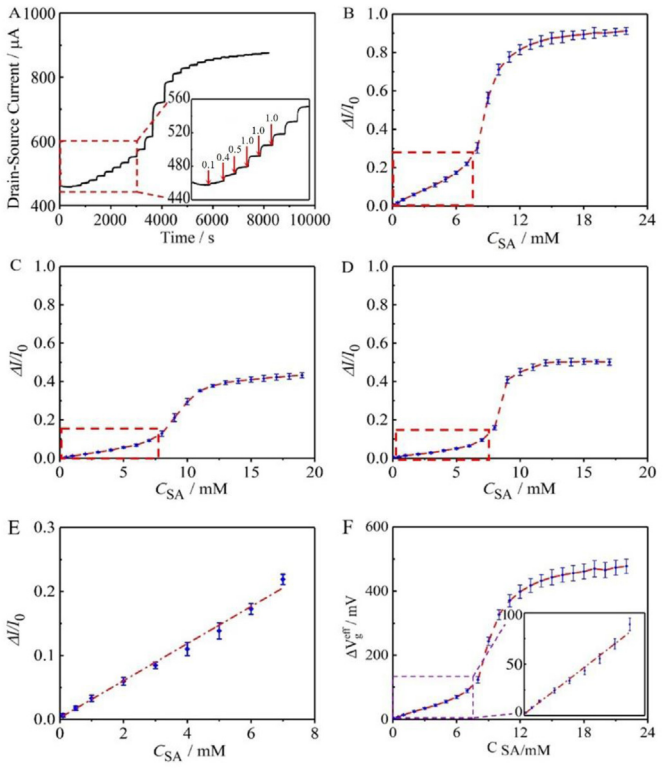

Fig. 4. (A) Drain-source channel current response to continuous addition of 0.1, 0.4, 0.5, 1.0, 1.0, … and 1.0 mM sialic acid in 10 mM pH 7.4 PBS with 9-mm^2 gate electrode at a gate voltage of 0.9 V. Inset: enlarged version at low SA concentrations. Plots of relative channel current change of the OECT-based biosensors with gate electrode area of (B) 9, (C) 1 and (D) 4 mm^2 *vs* SA concentration in 10 mM pH 7.4 PBS. (E) Plot of relative channel current change *vs* SA concentration, and the data are from (A). (F) Plot of change of effective gate voltage at 9-mm^2 biosensor *vs* SA concentration. Inset: SA concentration ranging from 0.1 to 7.0 mM.

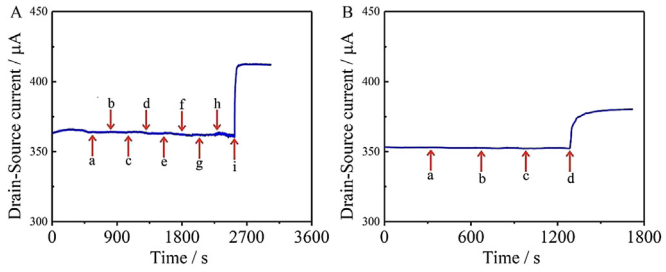

Fig. 5. (A) Responses of the OECT-based biosensor upon addition of 5 mM (a) glucose, (b) mannose, (c) lactose, (d) fructose, (e) sucrose, (f) maltose, (g) galactose, (h) ribose and (i) SA. (B) Responses of the OECT-based biosensor upon addition of (a) 5 μM DA, (b) 50 μM AA, (c) 300 μM UA and (d) 2 mM SA.

The drain-source channel current response of the OECT-based biosensor with gate electrode area of 9 mm^2 upon continuous addition of sialic acid was examined at the gate voltage of 0.9 V (Fig. 4A). After adding SA into PBS, the channel current increased immediately, indicating the rapid recognition process of APBA to SA. With the increasing SA concentration, the current continuously increased, and trended to a maximum value due to the saturated binding of the surface boronic acid by SA. Generally, the response of OECTs is proportional to the ratio of width to length of the channel and is sensitive to the gate voltage. To prove the response mechanism, three OECTs with the same *W*/*L* ratio and the gate electrode area of 9 mm^2, 4 mm^2 and 1 mm^2 were prepared for SA sensing (Fig. 4B, C and 4D). The OECT-based biosensor with the gate area of 9 mm^2 exhibited the maximum relative channel current change at different SA concentrations, which should be attributed to the more loading of CNTs along with the immobilized APBA for binding more SA on the surface of gate electrode, which led to larger increase of the electron transfer resistance and decrease of gate voltage between the electrolyte/channel and gate/electrolyte interfaces when it worked in non-Faradaic regime. Interestingly, the responses at all these biosensors showed abrupt increase when the SA concentration became higher than 7 mM and then trended to the maximum value at the SA concentrations higher than 12 mM, which led to similar sigmoid curve. The biosensor with the gate area of 9 mm^2 exhibited the linear response range in the concentration range from 0.1 mM to 7.0 mM ($R^2 = 0.999$) (Fig. 4E), which was located in the total SA content of 0.3 and 0.45 mM in urine samples for bladder tumor and glomerulonephritis, and 1.77–4.84 mM in serum samples for gastrointestinal tract, breast, chronic lymphocytic leukaemia, stomach, colorectal, gallbladder, thyroid, oral, endometrial and lung cancer, respectively [53]. Generally, the SA level of normal people is 1.6–2.9 mM [13], while in the serum samples of lung cancer patients it is higher than 3 mM [53]. Obviously, the proposed OECT-based biosensor could be used for direct detection of SA levels in practical serum samples of lung cancer patents. As mentioned above, the variation of drain-source channel current was caused by the change of the effective gate voltage (ΔVg^{eff}) owing to the specific binding of SA to APBA on gate electrode. The ΔVg^{eff} could be exacted from the current change and the transfer curve, and the ΔVg^{eff} towards the SA concertation exhibited the sigmoid curve, while the ΔVg^{eff} showed the linear response in the same concentration range from 0.1 to 7.0 mM with the slope of 11.37 mV/mM (Fig. 4F).

3.4. Selectivity of OECT-based biosensor

To ensure the practical application of the proposed biosensor, the recognition selectivity of APBA to SA was studied by the response of the biosensor to SA and different interferents. After 5 mM saccharides such as glucose, mannose, lactose, fructose, sucrose, maltose, galactose and ribose was added in the detection solution, respectively, the OECT-based biosensor showed negligible response, while the addition of SA led to obvious increase of channel current (Fig. 5A), confirming the recognition specificity between APBA and SA at pH 7.4 [54] on the gate surface and the selectivity of the designed biosensor toward SA. Considering the fact that many other physiological interferents such as dopamine (DA), ascorbic acid (AA) and uric acid (UA) exist in the serum samples, DA, AA, UA and SA at their natural concentrations [55,56] were added into PBS to simulate the practical serum environment. The designed biosensor did not show any response to these interferents under the optimized conditions (Fig. 5B).

3.5. Sample analysis

To evaluate the application potential of the proposed OECT-based biosensor, the detections of SA in practical serum samples of lung cancer patients and normal people were performed. After 50 μL10 mM pH 7.4 PBS and 10 μL serum sample were directly dropped on the OECT-based biosensor to incubate for 10 min, the drain-source channel current at a gate voltage of 0.9 V and a drain voltage of 50 mV was recorded, and the response at 300 s was collected. The results were compared with those from the commercial ELISA kit. As listed in Table 1, the OECT-based biosensor gave acceptable results with the relative errors ranging from 6.84 to 8.39%. Here, the detectable range of ELISA kit is 30–700 ng/L, which is far lower than the SA level in serum samples, thus the serum samples were million-fold diluted for ELISA test. The slight higher values obtained with the biosensor resulted from the dilution step in ELISA. Thus the proposed biosensor was an ideal platform for sialic measurement in clinical diagnosis.

4. Conclusions

This work designs a simple and convenient biosensing device for the detection of SA levels in serum samples. The OECT-based

Table 1
SA analysis in serum samples comparing with commercial ELISA kit.

Sample No.	Proposed method/mM	Reference method/mM	Relative error/(%)
1 (Lung cancer)	3.73	3.48	7.18
2 (Lung cancer)	3.97	3.68	7.88
3 (Lung cancer)	3.51	3.27	7.34
4 (Lung cancer)	4.72	4.39	7.52
5 (Lung cancer)	4.37	4.09	6.84
6 (Normal)	1.55	1.43	8.39
7 (Normal)	1.96	1.82	7.69
8 (Normal)	1.57	1.45	8.28
9 (Normal)	1.76	1.64	7.32
10 (Normal)	2.17	2.03	6.90

biosensor can be fabricated in batch by coating the gate electrode with carboxylated multi-wall carbon nanotubes and the general drain/source electrodes with PEDOT:PSS served as channel. After the recognition element APBA is covalently linked to the carboxyl group of carbon nanotubes, the obtained biosensor shows selective response to SA due to the increased electron transfer resistance and the decrease of gate voltage. The relative change of drain-source channel current shows a linear dependence on SA concentration ranging from 0.1 to 7 mM, which locates in the practical levels of SA in the samples from patients and normal people. The proposed biosensor possessed the potential as a new portable device for evaluation of SA levels in clinical diagnose.

CRediT authorship contribution statement

Lizhen Chen: Writing - original draft, Writing - review & editing. **Naixiang Wang:** Formal analysis. **Jie Wu:** Supervision. **Feng Yan:** Funding acquisition. **Huangxian Ju:** Funding acquisition, Writing - original draft, Writing - review & editing.

Declaration of competing interest

The authors declare that they have no known competing financial interests or personal relationships that could have appeared to influence the work reported in this paper.

Acknowledgement

We gratefully acknowledge the National Natural Science Foundation of China (21361162002, 21635005, 21827812, 21890741), and the Hong Kong Polytechnic University (Project No. G-SB51, 1-YW0Y).

References

[1] J. Dennis, I. Nabi, M. Demetriou, Metabolism, cell surface organization, and disease, Cell 139 (2009) 1229–1241.
[2] J.G. Gu, T. Isaji, Q.S. Xu, Y. Kariya, W. Gu, T. Fukuda, Y.G. Du, Potential roles of N-glycosylation in cell adhesion, Glycoconj. J. 29 (2012) 599–607.
[3] R. Haltiwanger, J.B. Lowe, Role of glycosylation in development, Annu. Rev. Biochem. 73 (2004) 491–537.
[4] K. Lau, J. Dennis, N-glycans in cancer progression, Glycobiology 18 (2008) 750–760.
[5] Y.L. Chen, L. Ding, H.X. Ju, In situ cellular glycan analysis, Acc. Chem. Res. 51 (2018) 890–899.
[6] H. Hisatoshi, N. Takashi, M. Nobuaki, J. Piao, O. Kazue, S. Sadanori, I. Shinichi, S. Naoya, T. Koichi, J. Furukawa, Sialic acid linkage specific derivatization of glycosphingolipid glycans by ring-opening aminolysis of lactones, Anal. Chem. 90 (2018) 13193–13199.
[7] Y. Rohan, M. Preeti, S. Balamurugan, T. Suraj, B. Harikrishna, V.M. Raghavendra, S. Sivakoti, K. Raghavendra, Imaging and targeting of the α(2-6) and α(2-3) linked sialic acid quantum dots in zebrafish and mouse models, ACS Appl. Mater. Interfaces 10 (2018) 28322–28330.
[8] Z.J. Zhang, W. Manfred, H. Stephanie, Serum sialylation changes in cancer, Glycoconj. J. 35 (2018) 139–160.
[9] M. Joshi, R. Patil, Estimation and comparative study of serum total sialic acid levels as tumor markers in oral cancer and precancer, J. Canc. Res. Therapeut. 6 (2010) 263–266.
[10] B. Christian, A. Marieke, H. Martijn, J. Gosse, Sialic acids sweeten a tumor's life, Canc. Res. 74 (2014) 3199–3204.
[11] O. Pearce, L. Heinz, Sialic acids in cancer biology and immunity, Glycobiology 26 (2016) 111–128.
[12] F. Montserrat, L. Esther, R. Manel, N.A. Rosa, S. Marc, C. Josep, L. Rafael, P. Rosa, Comparative study of blood-based biomarkers, 2,3-sialic acid, PSA and PHI, for high-risk prostate cancer detection, Int. J. Mol. Sci. 18 (2017) 845–856.
[13] K. Gopaul, M.A. Crook, Sialic acid: a novel marker of cardiovascular disease? Clin. Biochem. 39 (2006) 667–681.
[14] K. Tsuneo, A blood tumor marker combination assay produces high sensitivity and specificity for cancer according to the natural history, Cancer Med 7 (2018) 549–556.
[15] W. Przemyslaw, T. Emil, C. Robert, J.B. Jan, C. Halina, Sialic acids as cellular markers of immunomodulatory action of dexamethasone on glioma cells of different immunogenicity, Mol. Cell. Biochem. 455 (2019) 147–157.
[16] H. Aida, J. José, S. Eleazar, V. Jesús, V. Ekaterina, J. Miguel, R. Hugo, Diagnosis of breast cancer by analysis of sialic acid concentrations in human saliva by surface-enhanced Raman spectroscopy of silver nanoparticles, Nano Res 10 (2017) 3662–3670.
[17] T.X. Gong, Y. Cui, D. Goh, K.K. Voon, P.P. Shum, G. Humbert, J. Auguste, X.Q. Dinh, K.T. Yong, M. Olivo, Highly sensitive SERS detection and quantification of sialic acid on single cell using photonic-crystal fiber with gold nanoparticles, Biosens. Bioelectron. 64 (2015) 227–233.
[18] J. Titilope, C. Wilairat, P. Chatchai, R. Thitima, Colorimetric determination of sialic acid based on boronic acid-mediated aggregation of gold nanoparticles, Microchim. Acta 185 (2018) 409–416.
[19] X.J. Yang, L. Zhou, Y. Hao, B. Zhou, P.H. Yang, Erythrocytes-based quartz crystal microbalance cytosensor for in situ detection of cell surface sialic acid, Analyst 142 (2017) 2169–2176.
[20] S. Li, J.L. Liu, Y.L. Lu, L. Zhu, C.D. Li, L.J. Hu, J. Li, J. Jiang, S. Low, Q.J. Liu, Mutual promotion of electrochemical-localized surface plasmon resonance on nanochip for sensitive sialic acid detection, Biosens. Bioelectron. 117 (2018) 32–39.
[21] T. Abdellah, S. Dimitri, I. Apolline, R. Odile, P. Dominique, J. Benoist, Measurement of free and total sialic acid by isotopic dilution liquid chromatography tandem mass spectrometry method, J. Chromatogr. B 879 (2011) 3694–3699.
[22] J.N. Wang, S.P. Zhang, H. Dai, H.L. Zheng, Z.S. Hong, Y.Y. Lin, Dual-readout immunosensor constructed based on brilliant photoelectrochemical and photothermal effect of polymer dots for sensitive detection of sialic acid, Biosens. Bioelectron. 142 (2019), 111567-111563.
[23] T.L. Liu, B. Fu, J.C. Chen, Z.H. Yan, K. Li, A non-enzymatic electrochemical sensor for detection of sialic acid based on a porphine/graphene oxide modified electrode via indicator displacement assay, Electrochim. Acta 269 (2018) 136–143.
[24] F. Amin, N. Apon, K. Proespichaya, L. Warakorn, T. Panote, A conductive porous structured chitosan-grafted polyaniline cryogel for use as a sialic acid biosensor, Electrochim. Acta 130 (2014) 296–304.
[25] X. Guo, J. Liu, F.Y. Liu, F. She, Q. Zheng, H. Tang, M. Ma, S.Z. Yao, Label-free and sensitive sialic acid biosensor based on organic electrochemical transistors, Sensor. Actuator. B Chem. 240 (2017) 1075–1082.
[26] N.X. Wang, A.N. Yang, Y. Fu, Y.Z. Li, F. Yan, Functionalized organic thin film transistors for biosensing, Acc. Chem. Res. 51 (2019) 890–899.
[27] P. Lin, F. Yan, Organic thin film transistors for chemical and biological sensing, Adv. Mater. 24 (2012) 34–51.
[28] J. Rivnay, S. Inal, A. Salleo, R.M. Owens, M. Berggren, G.G. Malliaras, Organic electrochemical transistors, Nat. Rev. Mater. 3 (2018) 17086.
[29] N.X. Wang, Y.Z. Liu, Y. Fu, F. Yan, AC measurements using organic electrochemical transistors for accurate sensing, ACS Appl. Mater. Interfaces 10 (2018) 25834–25840.
[30] A. Campana, T. Cramer, Tobias, D.T. Simon, M. Berggren, F. Biscarini, Electrocardiographic recording with conformable organic electrochemical transistor fabricated on resorbable bioscaffold, Adv. Mater. 26 (2014) 3874–3878.
[31] X. Gu, C.L. Yao, Y. Liu, I.M. Hsing, 16-channel organic electrochemical transistor array for in vitro conduction mapping of cardiac action potential, Adv. Healthcare Mater. 5 (2016) 2345–2351.
[32] H. Felix, K. Jessica, C. Thanh, M. Walid, X. Lu, P. Vivek, S. Anna, T. Xuan, I. Sven, PEDOT:PSS organic electrochemical transistor arrays for extracellular electrophysiological sensing of cardiac cells, Biosens. Bioelectron. 13 (2017) 132–138.
[33] W. Lee, D. Kim, J. Rivnay, N. Matsuhisa, T. Lonjaret, T. Yokota, H. Yawo, M. Sekino, G.G. Malliaras, T. Someya, Integration of organic electrochemical and field-effect transistors for ultraflexible, high temporal resolution electrophysiology arrays, Adv. Mater. 28 (2016) 9722–9728.
[34] J. Jo, K. Kwon, Z. Khan, X. Crispin, T. Kim, Gelatin hydrogel-based organic electrochemical transistors and their integrated logic circuits, ACS Appl. Mater. Interfaces 10 (2018) 39083–39090.
[35] H. Tang, P. Lin, H.L.W. Chan, F. Yan, Highly sensitive dopamine biosensors based on organic electrochemical transistors, Biosens. Bioelectron. 26 (2011) 4559–4563.
[36] C.Z. Liao, C.H. Mak, M. Zhang, H.L.W. Chan, F. Yan, Flexible organic electrochemical transistors for highly selective enzyme biosensors and used for saliva testing, Adv. Mater. 27 (2015) 676–681.
[37] H. Tang, F. Yan, P. Lin, J.B. Xu, H.L.W. Chan, Highly sensitive glucose biosensors based on organic electrochemical transistors using platinum gate electrodes modified with enzyme and nanomaterials, Adv. Funct. Mater. 21 (2011) 2264–2272.
[38] A.N. Yang, Y.Z. Li, C.X. Yang, Y. Fu, N.X. Wang, L. Li, F. Yan, Fabric organic electrochemical transistors for biosensors, Adv. Mater. 30 (2018) 1800051.
[39] C.H. Mak, C.Z. Liao, Y. Fu, M. Zhang, C.Y. Tang, Y.H. Tsang, H.L.W. Chan, F. Yan, Highly-sensitive epinephrine sensors based on organic electrochemical transistors with carbon nanomaterial modified gate electrodes, J. Mater. Chem. C 3 (2015) 6532–6538.
[40] C. Xiong, Y. Wang, H. Qu, L.J. Zhang, L.Z. Qiu, W. Chen, F. Yan, L. Zheng, Highly sensitive detection of gallic acid based on organic electrochemical transistors with poly(diallyldimethylammonium chloride) and carbon nanomaterials nanocomposites functionalized gate electrodes, Sensor. Actuator. B Chem. 246 (2017) 235–242.
[41] L. Zhang, G.H. Wang, C. Xiong, L. Zheng, J.B. He, Y. Ding, S.H.B. Lu, G.B. Zhang, K. Chod, L.Z. Qiu, Chirality detection of amino acid enantiomers by organic electrochemical transistor, Biosens. Bioelectron. 105 (2018) 121–128.
[42] L. Kergoat, B. Piro, D.T. Simon, M. Pham, V. Noël, M. Berggren, Detection of

glutamate and acetylcholine with organic electrochemical transistors based on conducting polymer/platinum nanoparticle composites, Adv. Mater. 26 (2014) 5658–5664.
[43] O. Parlak, S. Keene, A. Marais, V. Curto, A. Salleo, Molecularly selective nanoporous membrane-based wearable organic electrochemical device for noninvasive cortisol sensing, Sci. Adv. 4 (2018), eaar2904.
[44] P. Lin, X.T. Luo, I.M. Hsing, F. Yan, Organic electrochemical transistors integrated in flexible microfluidic systems and used for label-free DNA sensing, Adv. Mater. 23 (2011) 4035–4040.
[45] Y. Fu, N.X. Wang, A.N. Yang, H.K.W. Law, L. Li, F. Yan, Highly sensitive detection of protein biomarkers with organic electrochemical transistors, Adv. Mater. 29 (2017) 1703787.
[46] R.X. He, M. Zhang, F. Tan, P.H.M. Leung, X.Z. Zhao, H.L.W. Chan, M. Yang, F. Yan, Detection of bacteria with organic electrochemical transistors, J. Mater. Chem. 22 (2012) 22072–22076.
[47] P. Lin, F. Yan, J.J. Yu, H.L.W. Chan, M. Yang, The application of organic electrochemical transistors in cell-based biosensors, Adv. Mater. 22 (2010) 3655–3660.
[48] D. Kim, N. Lee, J. Park, I. Park, J. Kim, H. Cho, Organic electrochemical transistor based immunosensor for prostate specific antigen (PSA) detection using gold nanoparticles for signal amplification, Biosens. Bioelectron. 25 (2010) 2477–2482.
[49] L.Z. Chen, Y. Fu, N.X. Wang, A.N. Yang, Y.Z. Li, J. Wu, H.X. Ju, F. Yan, Organic electrochemical transistors for the detection of cell surface glycans, ACS Appl. Mater. Interfaces 10 (2018) 18470–18477.
[50] D. Meenakshi, G. Dennis, An improved class of sugar-binding boronic acids, soluble and capable of complexing glycosides in neutral water, J. Am. Chem. Soc. 128 (2006) 4226–4227.
[51] E. Han, L. Ding, H.X. Ju, Highly sensitive fluorescent analysis of dynamic glycan expression on living cells using glyconanoparticles and functionalized quantum dots, Anal. Chem. 83 (2011) 7006–7012.
[52] G. Tarabella, C. Santato, S. Yang, S. Iannotta, G.G. Malliaras, F. Cicoira, Effect of the gate electrode on the response of organic electrochemical transistors, Appl. Phys. Lett. 97 (2010) 123304.
[53] P. Sillanaukee, M. Pönniö, I.P. Jääskeläinen, Occurrence of sialic acids in healthy humans and different disorders, Eur. J. Clin. Invest. 29 (1999) 413–425.
[54] H. Otsuka, E. Uchimura, H. Koshino, T. Okano, K. Kataoka, Anomalous binding profile of phenylboronic acid with N-acetylneuraminic acid (Neu5Ac) in aqueous solution with varying pH, J. Am. Chem. Soc. 125 (2003) 3493–3502.
[55] S.Y. Liu, F.P. Shi, X.J. Zhao, L. Chen, X.G. Su, 3-Aminophenyl boronic acid-functionalized $CuInS_2$ quantum dots as a near-infrared fluorescence probe for the determination of dopamine, Biosens. Bioelectron. 47 (2013) 379–384.
[56] A. Abellán, C. González, L. Vidal, A. Canals, E. Morallón, Portable electrochemical sensor based on 4-aminobenzoic acid-functionalized herringbone carbon nanotubes for the determination of ascorbic acid and uric acid in human fluids, Biosens. Bioelectron. 109 (2018) 123–131.